Joint Special Interest Group meeting between euspen and ASPE
Dimensional Accuracy and Surface Finish in Additive Manufacturing,
KU Leuven, BE, October 2017
www.euspen.eu

Measurement and characterisation of additively manufactured re-entrant surfaces

[1]Andrew Townsend, [1]Luca Pagani, [1]Paul J. Scott, [1]Liam Blunt

[1]*The Future Metrology Hub, University of Huddersfield, UK*

A.townsend@hud.ac.uk

Abstract
Additive manufacturing processes simultaneously present manufacturing and measurement challenges and opportunities. The as-built surface may contain *non-intentional* re-entrant (overhanging) features; however the AM process itself presents opportunities to *intentionally* produce re-entrant features. These features may be designed to improve component functionality in areas such as paint and coating adhesion, cell tissue osseointegration, electrical battery design, fluid flow and material cooling systems. These features may prove difficult or impossible to measure using conventional line-of-sight instrumentation. This paper reports on measurement of re-entrant features using X-ray computed tomography and the extraction of surface area and volume information from an additively manufactured planar surface and lattice structure. A parameter, intended to relate directly to functional performance, Sdr_{prime}, is introduced as the percentage of additional surface (including re-entrant surfaces) contributed by the texture as compared to a plane the size of the measurement area.

X-Ray computed tomography
Additive manufacturing
Re-entrant surfaces
Surface texture
ISO 25178

1. Introduction

Additive manufacturing (AM) techniques, particularly powder based processes, often produce surfaces with re-entrant features: undercuts and overhangs. This is an unintentional by-product of the layer-by-layer deposition process. However, one significant advantage AM systems have, when compared to conventional subtractive processes such as milling and turning, is the ability to manufacture components with *intentional*, designed-in, re-entrant features. These features would be tailored to the functional requirement of the component. Manufacturing components with these features will provide advantages based on two properties produced by such features; firstly, an increase in surface area for a given planar area and secondly the ability to mechanically *lock* to the re-entrant surface. Increased surface area for a given planer area may have applications in battery plate design where the surface contact area between liquid or gel electrolyte and the plate may be increased [1]. There may be applications in cooling and fluid flow where an increase in contact surface area provides greater volumetric efficiency [2]. Medical applications may include orthopaedic and dental implants where osseointegration between implant and tissue may be enhanced by the increased surface area [3]. These medical applications may also be enhanced by the second property that can be designed-in, the ability to mechanically *lock* to the surface. Examples of *lock* features due to mechanical design include architectural keystones used in masonry arches, dovetail joints used in woodworking and tooth preparation prior to application of an amalgam filling. During dental amalgam filling preparation the dentist drills a pocket with an internally widening taper or a shelf to prevent the filling loosening and falling out. The dental amalgam fills the pocket and is mechanically locked in place. AM processes allow generation of similar undercut features of different scales. In addition to medical applications of this *lock* feature, such as osseointegration, there are potential applications for this *lock* feature for paint and coating applications. Conventional measurement techniques, such as optical, stylus or CMM do not have the ability to measure re-entrant features or undercuts. X-ray computed tomography (XCT) has been used successfully for the measurement of internal surfaces [4, 5], dimensions [6, 7] and porosity [8]. There are no line-of-sight restrictions with XCT techniques. This paper reports on the measurement of two AM components: the as-built side surface of an AM medical implant and a section of a small lattice structure with nominally cylindrical lattice “bars”. The medical implant was manufactured from Ti6Al4V ELI using a Selective Laser Melting (SLM) system. The lattice was manufactured from Ti6Al4V ELI using an Electron Beam Melting (EBM) system. Methodology for the extraction and analysis of the surface data is reported for both samples. The applicability of areal surface texture data parameter generation per ISO 25178-2 is discussed. The results for generated data from the measured surfaces, including re-entrant features (mesh), is compared and contrasted to generated projected grid data to illustrate errors introduced when re-entrant features are not captured during the measurement and characterisation process. Parameter data for a sample designed re-entrant component will be discussed in section 3.

2. Methodology

The XCT measurement parameter settings and surface extraction procedure for the SLM planar surface and the EBM lattice are discussed in section 2.1. The data processing and parameter value extraction methods are reported in section 2.2.

2.1. Computed tomography measurements

The SLM planar surface and the EBM lattice were both measured using a Nikon XT H 225 CT. Reconstruction for both data sets was performed using Nikon CTPro 3D [9]. Surface determination and surface extraction was performed using VGStudio MAX 3.0 [10]. Local iterative surface determination was performed with a search distance of 4.0 voxels. The surface was extracted using the VGStudio MAX "Super Precise" setting. The XCT settings for the planar surface measurement are given in table 1. The extracted planar surface is shown in figure 1.

Table 1 XT H 225 measurement settings, SLM Ti6Al4V planar surface

Parameter	Value	Parameter	Value
Filter	1 mm Cu	Voxel size	7.1 µm
Acceleration voltage	160 kV	Detector size (pixels)	1008 x 1008
Filament current	62 µA	Number of projections	1583
Exposure time	2829 ms		

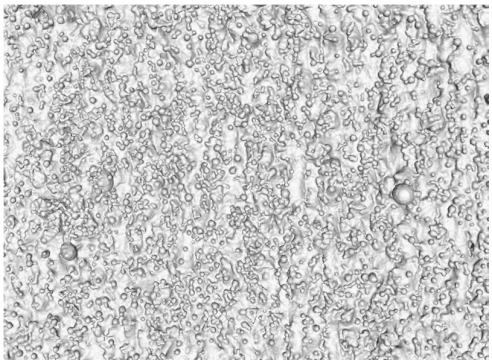

Figure 1. Extracted surface, SLM Ti6Al4V planar surface

The XCT settings for the lattice measurement are given in table 2. The extracted lattice surface is shown in figure 2. The region of interest (ROI) used in the surface evaluation is highlighted. All figures are in mm.

Table 2 XT H 225 measurement settings, EBM Ti6al4V ELI lattice

Parameter	Value	Parameter	Value
Filter material	None	Voxel size	3.6 µm
Acceleration voltage	60 kV	Detector size (pixels)	1008 x 1008
Filament current	100 µA	No. of projections	1583
Exposure time	1000 ms		

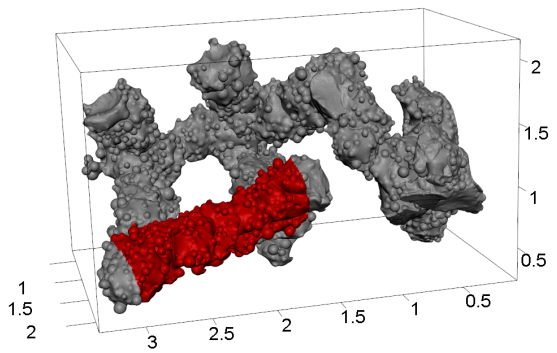

Figure 2. Extracted surface, EBM Ti6al4V ELI lattice, showing ROI.

2.2. Data processing and parameter extraction

Figures 4 and 5 show, respectively, the complete extracted SLM planar surface and a detail section. The least-squares datum plane can be seen in both figures.

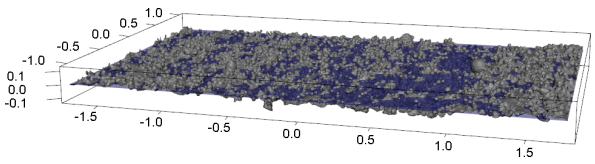

Figure 4. Planar surface showing datum plane

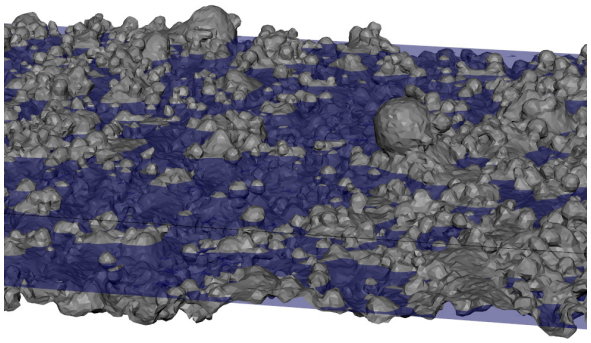

Figure 5. Detail of planar surface showing datum plane

The surface of the lattice section was unwrapped prior to analysis, see figure 6.

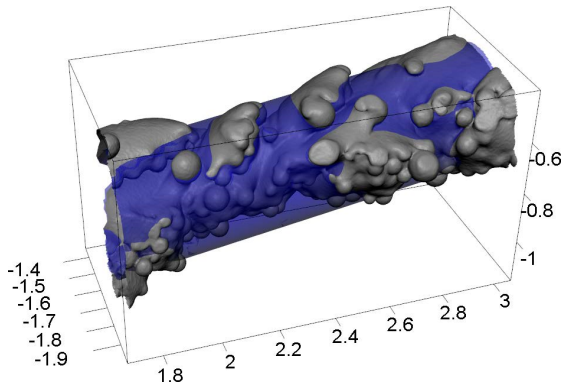

Figure 6. Extracted lattice ROI surface detail showing datum plane

Parameter data was extracted from a projected (grid) data set generated from the planar and lattice surfaces. Figure 7 shows a section of the unwrapped lattice. Projection of the surface onto a grid produces an interpolated surface *curtain* where the features are re-entrant. These areas can be seen in the figure. Surface area and volume data is caluclated from the grid projection using this information. The true surface area and volume, that is, including the re-entrant features, cannot be calculated from this projected data. This data set is similar to data sets generated by line-of-sight instruments such as optical focus variation and stylus profilometers. This grid parameter data was compared to values calculated from the mesh surface for both measurement samples. The mesh data analysis does include all surface feratures, re-entrant and non-re-entrant. In all cases, grid and mesh the primary surface is considered; no fitering has been applied to the surfaces.

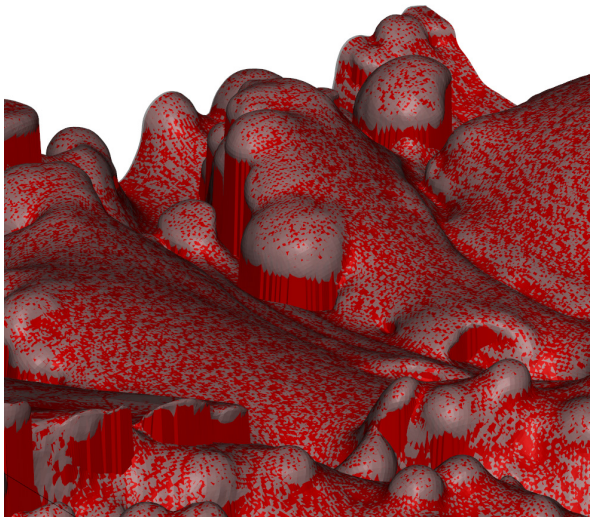

Figure 7. Unwraped lattice surface, showing interpolated grid *curtains*

Four parameters were extracted during the analysis: *Sdr*, Sdr_{prime}, *Vmc, Vvc*. These parameters where chosen because of their relevance to the functional perfomances discussed previously. The parameters relate to ISO 25178-2 parameters of the same name but, because of the nature of the mesh surface, are generated differently. The hybrid parameter *Sdr* is the developed interfacial area ratio. This is the percentage of addititional surface area contributed by the texture as compared to a plane the size of the *form* area (not the measurement area). The form area is the total area of all surfaces, including re-entrant surfaces, projected onto the datum plane. The form area is required for the calculation of surface parameters such as *Sa,* the arithmentic mean of the absolute of the ordinate value within the definition area (A). A parameter $\text{Sdr}_{\text{prime}}$ is introduced as the percentage of additional surface (including re-entrant surface) contributed by the texture as compared to to a plane the size of the *measurement* area. This number can be related directly to the ISO 25178-2 parameter *Sdr* and provides information directly related to surface function. Volume parameters *Vmc* and *Vvc* are core material volume and core void volume respectively. *Vmc* is defined here as the volume of material between 10% and 80% down from the maximum peak height to the maximum pit height. *Vvc* is the void volume (i.e. non-material volume) between 10% and 80% down from the maximum peak height to the maximum pit height.

Sdr is computed as

$$Sdr = \frac{1}{A}\left(\iint_{D_s}\left\|\mathbf{r}_u(u,v)\times\mathbf{r}_v(u,v)\right\|\,dudv - \iint_{D_{form}}\left\|\mathbf{r}_{form,u}(u,v)\times\mathbf{r}_{form,v}(u,v)\right\|\,dudv\right)$$

where $\mathbf{r}(u,v)$ is the measured surface, $\mathbf{r}_{form}(u,v)$ is the estimated form surface, A is the area of the form surface, $\mathbf{r}_\bullet(u,v)$ is the partial derivative in $\bullet$ direction, D_s is the domain of the measured surface and D_{form} is the domain of the form surface. Sdr_{prime} is similar to *Sdr* with exception that area A is replaced by A_{prime}, the projected area. The volume below the surface can be computed as

$$V = \iint_{\Sigma_{form}} \mathbf{r}_{sl}(u,v)\cdot\mathbf{n}_{form}(u,v) - Sv \;\; d\sigma_{form} \qquad (1)$$

where Σ_{form} is the form surface, $\mathbf{r}_{sl}(u,v)$ represents the scale limited surface, $\mathbf{n}_{form}(u,v)$ is the normal of the form surface and

$$d\sigma_{form} = \left\|\mathbf{r}_{form,u}(u,v)\times\mathbf{r}_{form,v}(u,v)\right\|\;\; dudv$$

is the infinitesimal area element. From Eq. 1 it is possible to compute the contribution of each height value to the total volume. This density function is expressed as $f_V(h)$. It should be noted that, since the surface in these applications includes re-entrant features this function will not be monotonically increasing, so it is not therefore possible to compute the volume parameter series according to ISO 25178-2. It is proposed to compute these parameters using the percentage of the height instead of area as used in the standard. Let $f_V(h^*)$ the density distribution of the volume as a function of the percentage of the height, a possible definition of $Vm(p)$, with $0 \le p \le 1$, can be

$$Vm(p) = \frac{Sz}{A_{\max}}\int_p^1 f_V(h^*)\;\; dh^*$$

while

$$Vv(p) = \frac{Sz}{A_{\max}}\int_0^p f_{V,\max}(h^*) - f_V(h^*)\;\; dh^*$$

where $A_{\max}$ is the maximum section area, $f_{V,\max}(h^*)$ is the maximum value of the density function and $h^* = \frac{h - Sv}{Sz}$. The core volume related parameters can be computed as

$$Vmc = Vm(q) - Vm(p) \quad Vvc = Vv(q) - Vv(p)$$

where p and q are percentages of the distance down from the maximum peak height to the maximum pit height, 10% and 80% respectively.

3. Results

3.1. Structured surface

Figure 10a shows a CAD representation of a sample structured surface, designed with intentional re-entrant features. The surface consists of repeated planar *mushroom* features, figure 10b. Each *mushroom* consists of a *cap* 2 x 2 x 2 mm³ (H x W x D) attached to a 2 x 1 x 1 mm³ *stem*. For calculation of *Sdr* from the mesh, for a single *mushroom* feature, including the base area directly below the *mushroom*, the area equivalent to the form area is 10 mm². This includes the top surface, 4 mm², and two horizontal areas of 3 mm² each: the underside of the mushroom cap and the base surface. This area is used to calculate *Sdr*. The plane area equivalent to the measurement area is 4 mm². This area is used to calculate Sdr_{prime}. The total feature surface area, including the base area directly below the *mushroom*, is 34 mm². The *Sdr* value would be (34-10) /10 x 100 = 240%. The Sdr_{prime} value would be (34-4) /4 x 100 = 750%. If a grid projection were used for surface reconstruction the *mushroom* would be evaluated to be a block 2 x 2 x 4 mm³ (this includes interpolated side *curtains*). The feature surface area would calculated as 36 mm², producing an *Sdr* value of 800%. This result illustrates that

the calculated surface when re-entrant features are included (34 mm²) may be *less* than the calculated surface when they are not included (36 mm²).

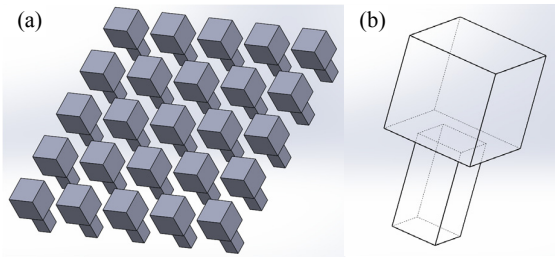

Figure 10. (a) structured surface and (b) single *mushroom* detail

The values for *Sdr* and Sdr_{prime} for the mesh and grid are shown in table 4, together with the values of volume parameters *Vmc* and *Vvc* for a core extending 10% down from the top surface (p=10%=0.4 mm) to 80% down from the top surface (q=80%=3.2 mm).

Table 4. Single planar *mushroom* extracted parameters

Method	*Sdr*	Sdr_{prime}	*Vmc*/ (mm³/mm²)	*Vvc*/ (mm³/mm²)
Mesh	240%	750%	1.9	0.9
Grid	800%	800%	2.8	0.0

The height vs volume curve is shown in figure 12 and the material ratio curve is shown in figure 13.

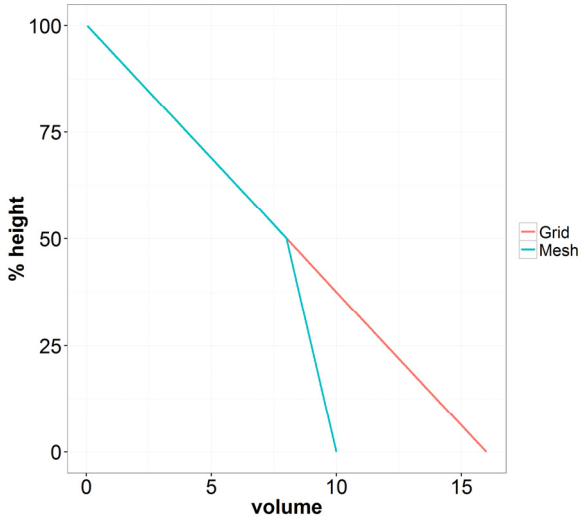

Figure 12. Height vs volume curve, single structured *mushroom*

The knee in the curve for the mesh is located at the 50% height, where the shape transitions from *cap* to *stem*. The grid projection produces a straight line as the transition is not measured. The calculated volumes for the entire feature (100% volume on the material ratio curve) are 10 mm³ for the mesh and 16 mm³ for the grid projection.

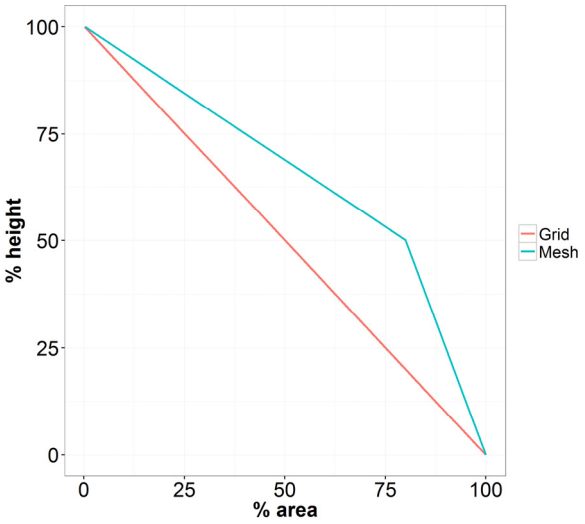

Figure 13. Material ratio curve, single structured *mushroom*

3.2. SLM planar surface

Table 3 shows the values of *Sdr*, Sdr_{prime}, *Vmc* and *Vvc* for mesh and grid for the SLM planar surface.

Table 3 SLM planar surface texture parameters

Method	*Sdr*	Sdr_{prime}	*Vmc*/ (mm³/mm²)	*Vvc*/ (mm³/mm²)
Mesh	55%	79%	0.076	0.0042
Grid	68%	68%	0.077	0.0038

The material ratio curve for the planar surface is shown in figure 14. The difference in the developed area interfacial area ratio, *Sdr* between grid and mesh for the SLM planar surface is 13%. The difference for Sdr_{prime} is -11%. The difference between grid and mesh for the volume parameters, *Vmc* and *Vvc,* is approximately 1% and -10%.

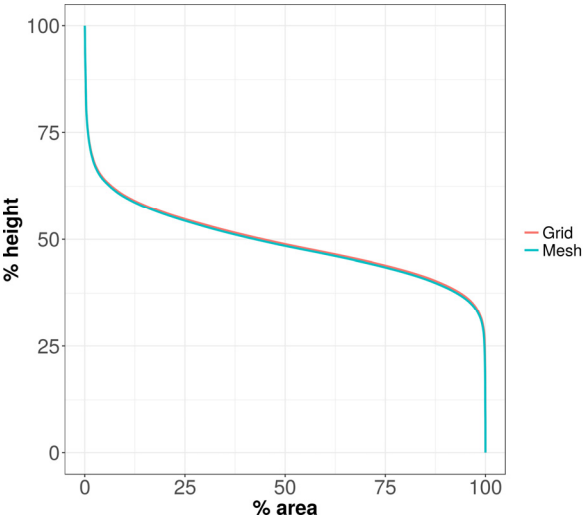

Figure 14. Matrial ratio curve, SLM planar surface

3.3. Lattice structure

Table 4 shows the values of *Sdr, Sdr_{prime}, Vmc* and *Vvc* for mesh and grid for the EBM lattice surface.

Table 4 EBM lattice surface texture parameters

Method	*Sdr*	Sdr_{prime}	*Vmc*/ (mm^3/mm^2)	*Vvc*/ (mm^3/mm^2)
Mesh	42%	55%	0.064	0.018
Grid	49%	49%	0.077	0.028

The material ratio curve for the lattice structure is shown in figure 15. The difference in the developed area interfacial area ratio, *Sdr* between grid and mesh for the EBM lattice surface is 7%. The difference for Sdr_{prime} is -6%. The difference between grid and mesh for the volume parameters, *Vmc* and *Vvc* is approximately 20% and 56%.

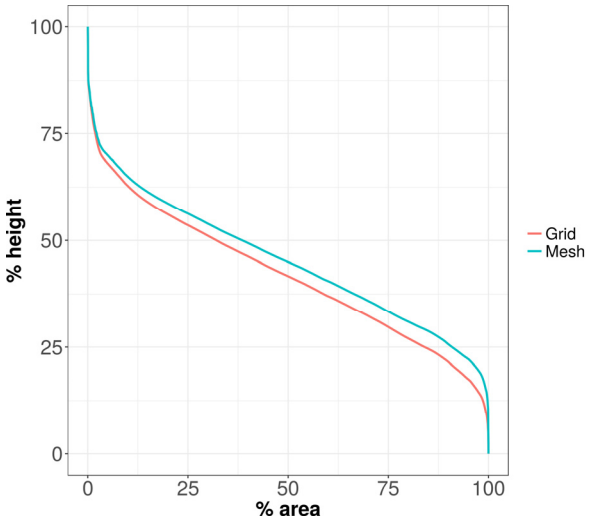

Figure 15. Material ratio curve, EBM lattice

4. Conclusions

AM processes provide the ability to produce complex freeform surfaces and re-entrant features that enhance component functionality, from bio-attachment, battery design, cooling systems, paint and coating adhesion. The ability to measure and characterise these surfaces accurately will be the key to performance optimisation. These surfaces present measurement and data analysis challenges that require the ability to image and extract meaningful data from a complex point clouds or meshes rather than a uniform grid typically generated by line-of-sight instrumentation processes. A method for extraction of surface texture parameters from re-entrant AM surfaces has been demonstrated. XCT measurements scans of two AM surfaces have been made, capturing data for surfaces that would prove difficult or impossible to capture using line-of-sight measurements. Actual surface area and volume data has been extracted and compared to projected (grid) areas and volumes for this data. An example generated structured surface has been discussed. A new parameter, Sdr_{prime} has been suggested. This parameter is the percentage of additional surface (including re-entrant surfaces) contributed by the texture as compared to a plane the size of the measurement area. This new parameter was developed to provide a direct relation to functional performance in applications where the actual surface area is important. There are significant errors in volume (up to 56% for *Vvc*) and area (up to 11% for Sdr_{prime}) when re-entrant features of as-built SLM and EBM additively manufactured components are not measured and included in analyses. Including re-entrant features, using the techniques presented here, will provide more accurate data required for analysis and optimisation of the functional performance of AM components.

References

[1] Gyenge E, Splinter S, Jung J, Snaper A 2002 High-specific surface area, three-dimensional reticulated electrodes for deep cycle lead-acid batteries. in *Seventeenth Annual Battery Conference on Applications and Advances. Proceedings of Conference (Cat. No.02TH8576)*

[2] Silk E A, Kim J, and Kiger K 2006 Spray cooling of enhanced surfaces: impact of structured surface geometry and spray axis inclination. *International Journal of Heat and Mass Transfer.* **49**(25): p. 4910-4920

[3] Rungsiyakull C, Li Q, Sun G, Li W, Swain M V 2010 Surface morphology optimization for osseointegration of coated implants. *Biomaterials.* **31**(27): p. 7196-7204

[4] Townsend A, Pagani L, Blunt L, Scott P J, Jiang X 2017 Factors affecting the accuracy of areal surface texture data extraction from X-ray CT. *CIRP Annals - Manufacturing Technology*

[5] Thompson A, Korner L, Senin N, Lawes S, Maskery I, Leach R K 2017 Measurement of internal surfaces of additively manufactured parts by X-ray computed tomography. in *7th Conference on Industrial Computed Tomography*. Leuven, Belgium

[6] Müller P, Cantatore A, Andreasen J L, Hiller J, De Chiffre L 2013 Computed tomography as a tool for tolerance verification of industrial parts. *Procedia CIRP.* **10**: p. 125-132

[7] Kruth J P, Bartscher M, Carmignato S, Schmitt R, De Chiffre L, Weckenmann A 2011 *C*omputed tomography for dimensional metrology. *CIRP Annals-Manufacturing Technology*. **60**(2): p. 821-842

[8] Wits W W, Carmignato S, Zanini F, and Vaneker T H, 2016 Porosity testing methods for the quality assessment of selective laser melted parts. *CIRP Annals-Manufacturing Technology.* **65**(1): p. 201-204

[9] Nikon metrology NV, *Nikon CT-Pro*

[10] Volume Graphics GmbH, *VGStudio MAX*